Physics Letters B 269 (1991) 465–476
North-Holland

PHYSICS LETTERS B

A parametrization of $\sigma_T(\gamma^* p)$ above the resonance region for $Q^2 \geqslant 0$

H. Abramowicz [a], E.M. Levin [b,1], A. Levy [b,2] and U. Maor [c]

[a] *Institute of Experimental Physics, Warsaw University, PL-00 681 Warsaw, Poland*
[b] *Deutsches Elektronen-Synchrotron, DESY, W-2000 Hamburg, FRG*
[c] *School of Physics, Tel Aviv University, Tel Aviv 69978, Israel*

Received 17 July 1991

A smooth description of the total γ^* p cross section from the deep inelastic scattering region to the real photoproduction limit is obtained with a parametrization based on a Regge type approach. The parametrization is obtained from a fit to the structure function data of BCDMS, SLAC and NA28 and the available total photoproduction cross section measurements above the resonance region, $W > 1.75$ GeV. The fit gives a reliable description of the data and provides a smooth transition from photoproduction to the deep inelastic region. Together with an earlier parametrization of the resonance region, it can be used to estimate radiative corrections over the full kinematical range.

1. Introduction

The aim of this study is to present a phenomenological and numerical description of the cross sections for photon–proton interactions in the whole range of photon virtualities, from $Q^2 = 0$ to the highest Q^2 values available experimentally. From a purely practical point of view a parametrization of the γp cross section in a large range of Q^2, starting from the real photon cross section, is very useful for estimating acceptance corrections and radiative corrections for all experiments on leptoproduction.

From the theoretical point of view it is of interest to see whether experimentally the interactions of virtual photons of small virtuality display similar properties as hadron–hadron interactions. The possibility of a unified description of the small (soft processes) and high (hard processes) virtuality" photoproduction" cross sections may shed some light on the transition between the soft strong interactions and the hard interactions described in terms of perturbative QCD.

There are basically two main physical ideas behind the description of high energy strong interactions. The first one makes a distinct separation between the deep inelastic scattering (DIS) and the soft processes. Soft interactions can be thought of as being governed by special confinement forces which act at large distances, while typical hard processes such as DIS are well described by perturbative QCD. In the low x region, however, the study of DIS reveals properties similar to that of soft interactions. A good example is provided by the fact that the total cross section for absorption of virtual photons grows rapidly as $x \to 0$ and becomes compatible with the geometrical size of hadrons. Shadowing observed on nuclear targets at low x and up to relatively high Q^2 [1] is another manifestation of a property typical for soft processes. A similar type of shadowing is expected theoretically in the nucleon case at low x and high Q^2, where parton densities become very large, and it cannot be explained by miraculous confinement forces which would restore unitarity. Clearly the separation into soft and hard processes through confinement does not solve all problems, since we are faced with soft interactions also in typical hard processes such as DIS. It is thus not unnatural to expect a smooth transition from soft to hard processes. This is the essence of the second picture underlying strong interactions, which

[1] On leave from St. Petersbourg Nuclear Physics Institute, SU-188 350 Gatchina, USSR.
[2] On leave from School of Physics, Tel Aviv University, Tel Aviv 69978, Israel

we shall try to illustrate in the approach presented in this paper.

2. Phenomenology

It has been shown in ref. [2] that the total γp photoproduction cross section can be well described by the exchange of a pomeron and a reggeon trajectory:

$$\sigma_{\rm tot}(\gamma p)=\sigma^0_{I\!P} s^{\alpha_{I\!P}-1}+\sigma^0_{I\!R} s^{\alpha_{I\!R}-1} \quad (1)$$

where s is the center of mass energy squared, and $\alpha_{I\!P}$ and $\alpha_{I\!R}$ denote the pomeron and reggeon intercepts, respectively. The value of $(\alpha_{I\!P}-1)$ is expected to be small and positive while $\alpha_{I\!R}$ is about 0.5. It has been pointed out [3] that the cross section for virtual photon–proton scattering can be described in a similar Regge language, provided threshold effects arising from the presence of a virtual particle in the scattering process are taken into account.

The success of these two approaches led us to believe that one could find a parametrization based on a Regge type of approach which would account for both the real and the virtual photon absorption cross section.

In the deep inelastic region, the Regge language can be translated into the parton language, in the sense that the sea content of the proton determines the pomeron contribution to the absorption cross section and the valence content of the proton determines that of the reggeon. Thus, the total absorption cross section for virtual photon, γ*, scattering off the proton can be written as a sum of two contributions:

$$\sigma_{\rm tot}(\gamma^* p)=\sigma^*_{I\!P}(Q^2)+\sigma^*_{I\!R}(Q^2) \quad (2)$$

Notice that the low Bjorken x region of the parton language corresponds to large energies s and small virtualities Q^2, a region relevant for the application of the Regge language.

The relation between the total nucleon absorption cross section of transversely polarized virtual photons and the nucleon structure function F_2 is the following:

$$\sigma_{\rm T}(\gamma^* p)=\frac{4\pi^2\alpha}{Q^2}\frac{1}{1-x}\left(1+\frac{4m_p^2x^2}{Q^2}\right)\frac{1}{1+R(x,Q^2)} \times F_2(x,Q^2)\,, \quad (3)$$

where x and Q^2 are the usual variables used in the description of DIS processes, m_p is the proton mass, $R(x, Q^2)$ determines the relation between the nucleon structure functions F_2 and $2xF_1$ and measures the level of violation of the Callan–Gross relation. This cross section is relevant for the comparison with the real photon cross section, as real photons are only transversely polarized.

It has been known for a while [4] that the parton distributions in the nucleon, and thus the structure function F_2, can be well parametrized by an expression of the type

$$F_2 \sim x^a(1-x)^b\,, \quad (4)$$

where both a and b are functions of a variable t defined as follows:

$$t=\ln\left(\frac{\ln(Q^2/\Lambda^2)}{\ln(Q_0^2/\Lambda^2)}\right). \quad (5)$$

Here Λ is the QCD cutoff parameter and Q_0^2 is the scale at which one defines the initial conditions for perturbative QCD to be applicable in the nucleon case. In the QCD analysis of existing experimental data, Q_0^2 is usually taken to be 4 GeV^2.

Since for large s, $x\to Q^2/s$, and since the term $(1-x)^b$ can be thought of as a kinematical threshold factor (as only part of the total γp phase space is available for parton interactions), the expression (4) looks similar to the Regge type of expression with a being proportional to the relevant intercept [5]. We thus assume that F_2 can be decomposed into two terms, one related to pomeron exchange and the other to reggeon exchange,

$$F_2=F_2^{I\!P}+F_2^{I\!R}\,, \quad (6)$$

with each of them expressed as follows:

$$F_2^{\rm r}=C_{\rm r}(t)x^{a_{\rm r}(t)}(1-x)^{b_{\rm r}(t)}\,, \quad (7)$$

where r stands either for the pomeron $I\!P$ or the reggeon $I\!R$ and $C_{\rm r}$ represent the normalization factors.

A few comments are in order. There are at least two arguments against using an approximation of the type $x^{a(t)}$ for the small x behavior of structure functions. The first, demonstrated by Lopez and Yndurain [5] and also Martin [6], is that QCD evolution equations require in such an approximation a to be Q^2 independent as $x\to 0$. The other is that in the limit

of $x \to 0$ the solution of the QCD evolution equations behaves as [7,8]

$$F_2 = \frac{1}{Q^2} \exp\left(\sqrt{\frac{16N_c}{b} \ln\ln\frac{Q^2}{\Lambda^2} \ln\frac{1}{x}}\right), \tag{8}$$

where N_c is the number of colors and

$$b = \tfrac{11}{3}N_c - \tfrac{2}{3}n_f, \tag{9}$$

with n_f the number of flavors. This behavior cannot be easily reduced to a power like dependence of F_2 on x. On the other hand, shadowing corrections to parton distributions at low x may change crucially the x and Q^2 dependence of F_2, and the conclusion drawn by ref. [5] may not be valid.

Thus, although there is no strong argument for using a parametrization of the type (7), it can be treated as a simple approximation which could be valid in a limited range of x. This is similar to the case of the energy dependence of the γp cross section, where there are no strong arguments for the Regge type of behavior with a power law for the pomeron contribution and yet it is consistent with the data [2]. A clear advantage is that the structure of the $\sigma_T(\gamma^* p)$ remains the same as that of σ_T for real photons.

In order for formula (3) to describe the γp cross section both at $Q^2 = 0$ and for $Q^2 > 0$, an appropriate choice of variables is needed. Although at $Q^2 = 0$ gauge invariance requires $F_2(x, Q^2) = 0$ and thus formula (3) remains valid, it is not appropriate for numerical applications. The solution to this problem [9,10] is to introduce a mass scale, m_0, in such a way that the cross section remains $\sim 1/Q^2$ at large Q^2, and Q^2 independent at low Q^2. We thus replace the term

$$\frac{4\pi^2\alpha}{Q^2} \to \frac{4\pi^2\alpha}{Q^2 + m_0^2}. \tag{10}$$

The physical meaning of m_0^2 is that of the typical size of a real photon, or even better, that of the typical size of partons inside a real photon.

The next problem encountered in the application of formula (3) to the real photon data is related to the energy variables. While the real photon data are governed by s, the deep inelastic data are described in terms of x, with x defined through the following relation:

$$\frac{1}{x} = 1 + \frac{W^2 - m_p^2}{Q^2}, \tag{11}$$

where W^2 is the invariant mass squared of the hadronic system and corresponds to s for real photon interactions.

In order to retain a consistency between the Regge picture and the parton language, it is useful to refer back to the underlying microscopic picture for reggeon exchange which is described by a simple ladder multiperipheral diagram. While in the Regge phenomenology the ladder diagram is described in the $g\phi^3$ theory where ϕ stands for a scalar meson, in QCD the lines represent gluons. The general property of such a diagram is that for large Q^2 the cross section can be written as a series expansion in $\ln 1/x$:

$$\sigma \sim \frac{1}{Q^2} \sum c_n \left(\alpha_s \ln\frac{1}{x}\right)^n. \tag{12}$$

However, for $Q^2 \to 0$, the same diagram leads to

$$\sigma \sim \frac{1}{m_r^2} \sum c_n \left(\alpha_s \ln\frac{s}{m_r^2}\right)^n, \tag{13}$$

where the inverse of m_r^2 is the size of the target [8,11]. Taking into account the properties described above we choose for the energy variable

$$\frac{1}{x_r} = 1 + \frac{W^2 - m_p^2}{Q^2 + m_r^2}, \tag{14}$$

where m_r is the mass scale, typical for γp interactions. In the limit of $Q^2 \gg m_r^2$

$$x_r \to x \tag{15}$$

as required, and in the limit of $Q^2 \to 0$ and large W (large s)

$$x_r \to \frac{m_r^2}{W^2} = \frac{m_r^2}{s}. \tag{16}$$

For our particular problem, since we are dealing with pomeron and reggeon exchanges, we introduce two mass scales, $m_{I\!P}$ and $m_{I\!R}$, and thus two variables $x_{I\!P}$ and $x_{I\!R}$ respectively with

$$\frac{1}{x_{I\!P}} = 1 + \frac{W^2 - m_p^2}{Q^2 + m_{I\!P}^2} \tag{17}$$

and

$$\frac{1}{x_{I\!R}} = 1 + \frac{W^2 - m_p^2}{Q^2 + m_{I\!R}^2}. \tag{18}$$

The energy dependence in the Regge approach is re-

placed by the inverse of those variables. The final formula that we fit to the data is as follows:

$$\sigma_T(\gamma^{(*)}p)=\frac{4\pi^2\alpha}{Q^2+m_0^2}\frac{1}{1-x}\left(1+\frac{4m_p^2Q^2}{(Q^2+W^2-m_p^2)^2}\right)\times(F_2^{\mathcal{P}}+F_2^{\mathcal{R}}), \quad (19)$$

where

$$F_2^{\mathcal{P}}=C_{\mathcal{P}}(t)x^{a_{\mathcal{P}}(t)}(1-x)^{b_{\mathcal{P}}(t)}, \quad (20)$$

$$F_2^{\mathcal{R}}=C_{\mathcal{R}}(t)x^{a_{\mathcal{R}}(t)}(1-x)^{b_{\mathcal{R}}(t)} \quad (21)$$

and we redefine t so as to make it applicable also at $Q^2=0$,

$$t=\ln\left(\frac{\ln[(Q^2+Q_0^2)/\Lambda^2]}{\ln(Q_0^2/\Lambda^2)}\right). \quad (22)$$

Note that $1-x$, where x is defined by eq. (11), is equal to 1 at $Q^2=0$, and does not need to be redefined.

3. Data

We have used the available total γp cross section data above $W=1.75$ GeV to avoid the resonance region. For γ*p interactions we have used the NA28 [12] and the BCDMS [13] data on μp scattering and the SLAC [14] data on ep scattering. The kinematical range in the $1/x$ and Q^2 plane covered by these data is presented in fig. 1. The NA28 experiment has measured the nucleon structure function F_2 in μd interactions. In order to infer from the data the proton structure function we have used the measurement of F_2^n/F_2^p performed by the NM Collaboration [15] over a large x and Q^2 range. We have used formula (3) to transform the data on F_2 into $\sigma_T(\gamma^*p)$. In order to do so we have relied on the measurement of R performed by SLAC [14,16] and their parametrization based on all existing data and claimed to be valid above $Q^2=0.3$ GeV^2.

4. Fitting procedure

The fitting procedure consisted of two steps. In the first step formula (19) was fitted to the data on the absorption cross section for transversely polarized real and virtual photons. In the second step, we have performed a separate fit to $\sigma_T(\gamma^*p)(1+R)$, which depends only on the measurements of F_2. If not for numerical uncertainties, the ratio of the results obtained in those fits could in principle shed some light on

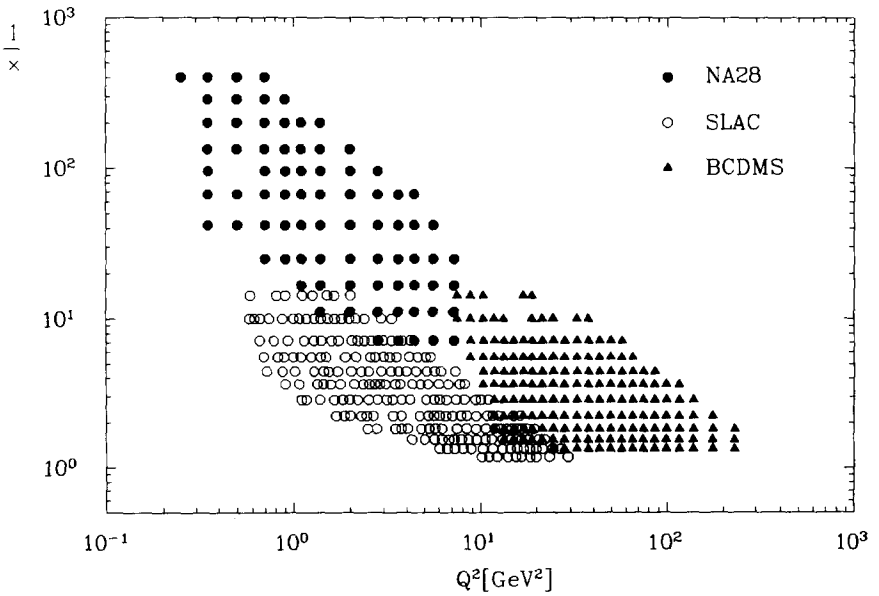

Fig. 1. Kinematical range in $1/x$ and Q^2 covered by deep inelastic scattering data.

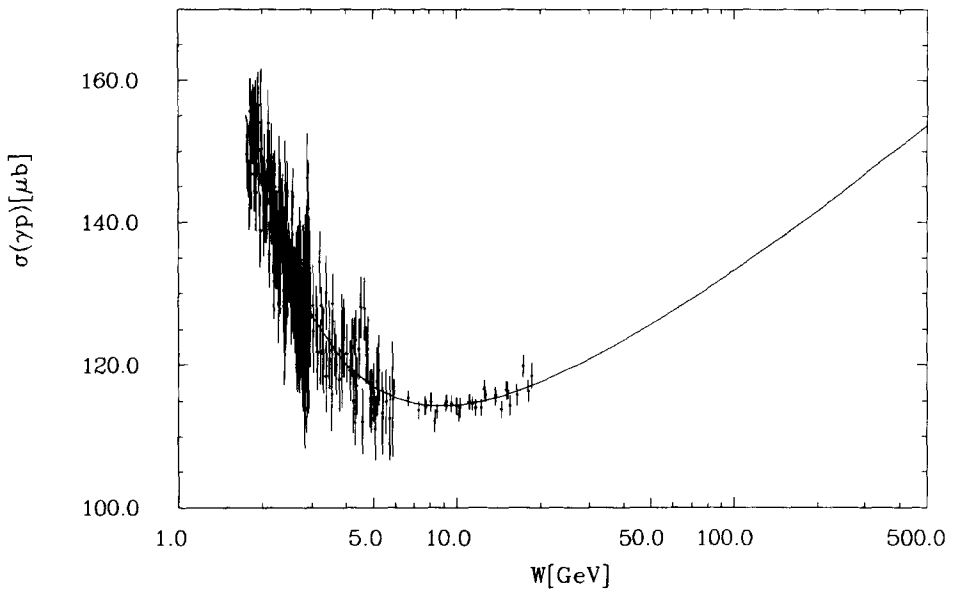

Fig. 2. Comparison between the total γp cross section as measured for the real photon and the results of the fit, presented as a function of the center of mass energy W.

the value of R in the region not yet accessible experimentally.

The results of our fits required a distinction between the parameters $C_{\mathbb{P}}$, $b_{\mathbb{P}}$, $a_{\mathbb{R}}$ and $b_{\mathbb{P}}$ which increase with Q^2 and were assumed to be of the form

$$p(t)=p_1+p_2 t^{n} \tag{23}$$

and $C_{\mathbb{P}}$ and $a_{\mathbb{P}}$, both decreasing functions of Q^2, which were assumed in the form

$$p(t)=p_1+(p_1-p_2)\left(\frac{1}{1+t^{n}}-1\right). \tag{24}$$

Since there are no data available for $Q^2>250$ GeV^2, the form of eq. (24) ensures that p_2, the limiting value of $p(t)$ when $t\to\infty$, can be constrained to physical values. In the case of $C_{\mathbb{P}}$, p_2 is required to be nonnegative, while for $a_{\mathbb{P}}$ p_2 is required to be bigger than -1, a limit expected from QCD [17,18].

All together there were 694 data points and 23 free parameters, including 3 mass scales – m_0^2, $m_{\mathbb{P}}^2$ and $m_{\mathbb{R}}^2$, Q_0^2 and Λ^2 and 18 parameters describing the pomeron and reggeon terms.

In order to speed up the convergence of the fit the following procedure was adopted. First only the real photon data were fitted in order to determine the starting values for the three mass scales and $C_{\mathbb{P}}^1$, $C_{\mathbb{R}}^1$, $a_{\mathbb{P}}^1$ and $a_{\mathbb{R}}^1$. The next step was to fix these parameters and determine the other terms by using all the DIS data. Once a good fit was achieved all parameters were allowed to vary and a global fit was performed on the complete set of data. We have also allowed for a variation of the normalization of the NA28 and BCDMS data relative to the SLAC data. We found that an overall 2.5% increase of the NA28 measurement, well within the 7% normalization uncertainty quoted by the experiment, improves the χ^2. (The same result was found in another attempt to parametrize the same set of data on DIS [19]). For the sake of the fit, statistical and systematic errors were added in quadrature. For 694 data points and 24 free parameters (including the rescaling of the NA28 data) we find a total χ^2 of 661, equivalent to $\chi^2/\mathrm{ndf}=0.98$. The comparison between the data and the curves obtained from the fit are shown in fig. 2 for the real photon cross section and in fig. 3 for $F_2/(1+R)$. In order to obtain a parametrization of $\sigma_T(\gamma^*p)(1+R)$, we have fitted the data on F_2, keeping most of the parameters not involving t as well as Λ fixed at the values determined previously. We have

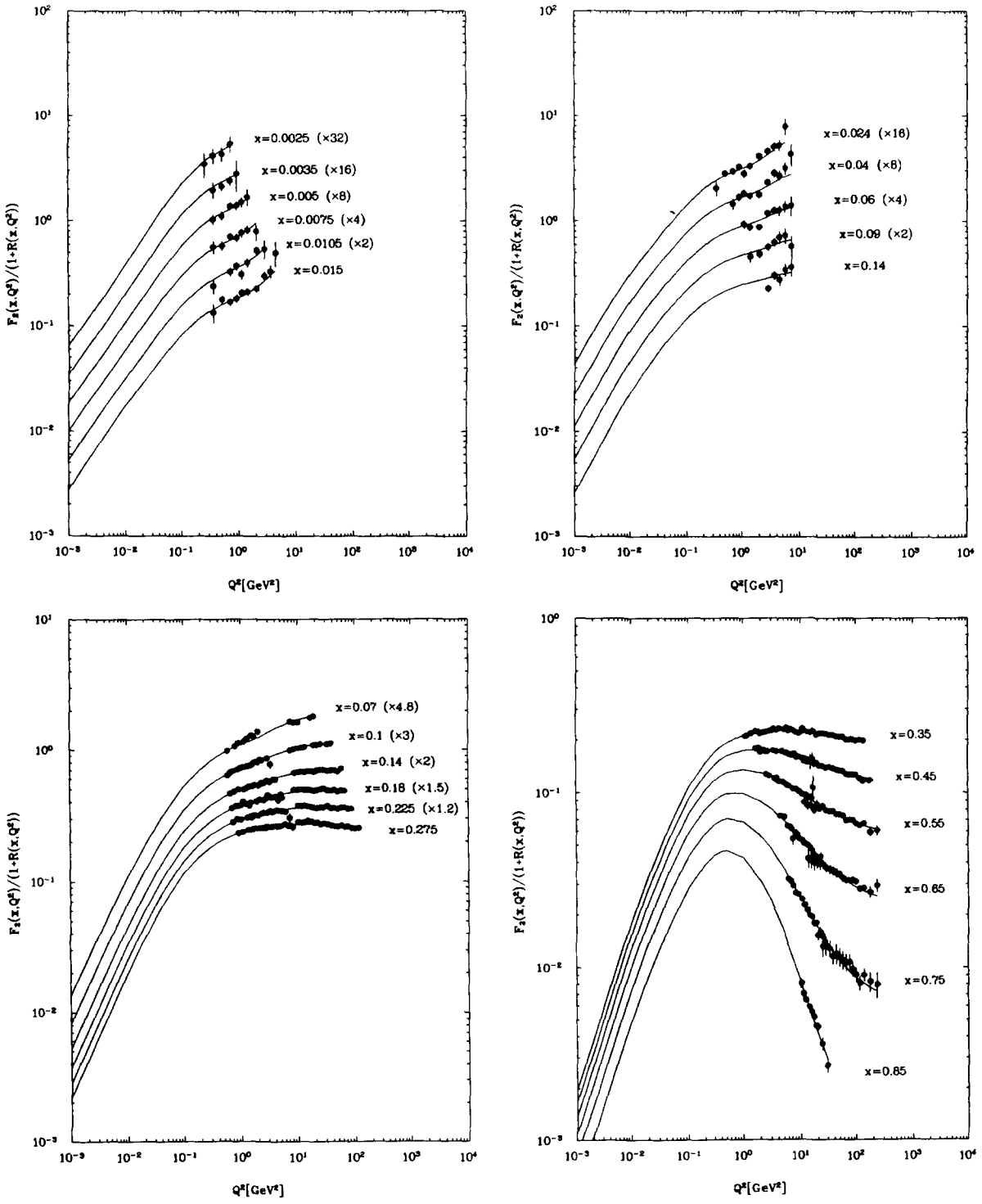

Fig. 3. Comparison between $F_2(x, Q^2)/[1+R(x, Q^2)]$ from the data and the results of the fit, for various constant values of x as a function of Q^2.

allowed all parameters describing $b_{\mathbb{P}}(t)$, $b_{\mathbb{R}}(t)$ and Q_0^2 to vary, assuming that F_2 may be affected by non-perturbative effects differently from $2xF_1$. In this case, for 467 data points and 15 free parameters we obtain a χ^2 of 410, equivalent to $\chi^2/\mathrm{ndf}=0.91$. We have also tried the inverse procedure, in which the real photon data and the F_2 data were fitted first and then only the F_2 data corrected by the $(1+R)$ term. The results were in agreement with the procedure described above.

5. Results

The results of our fits are presented in table 1. The error analysis for this large amount of parameters is very involved. We have checked that, for fixed values of Λ, the values of the mass scales vary within about 25%, while all the other parameters vary within 15 to 30%. The interesting observation is that both $a^1_{\mathbb{P}}$ and $a^1_{\mathbb{R}}$ are consistent with the expectation for the intercepts of the appropriate trajectories. Also the value of Λ of 255 MeV is compatible with values previously obtained in the standard QCD analysis of structure functions. It seems thus that one can extrapolate smoothly from $Q^2=0$ to higher values of Q^2 without loosing the nice interpretation valid for real photons and the QCD interpretation for high Q^2.

In the parton model the relation between the absorption cross section and the nucleon structure function is described by eq. (3) with F_2 depending only on x. The relatively small value of $m_0^2=0.3$ GeV^2, implies that the parton language can be applied already at low values of Q^2, but the large value of $m^2_{\mathbb{P}}=10$ GeV^2 introduces scaling violation of F_2 even at large values of Q^2. The Q^2 dependence of F_2 induced by the presence of $m_{\mathbb{P}}$ is typical for higher twist effects. Judging from the value of $Q_0^2=0.3$ GeV^2, QCD should be applicable at low Q^2, but again the large value of $m^2_{\mathbb{P}}$ indicates that higher twist effects are important even at relatively high Q^2. Our result, that $m^2_{\mathbb{P}}$ is much bigger than $m^2_{\mathbb{R}}$, indicates that higher twist effects affect the sea (pomeron) contribution in a larger Q^2 domain than the valence (reggeon) contribution. The higher twist contribution to F_2 from the pomeron is negative due to the negative sign of $a_{\mathbb{P}}$, while that of the reggeon is positive but small. The importance of higher twist effects in the sea contribution has been pointed out by Donnachie and Landshoff [20].

We have checked that our parametrization extrapolates smoothly into the resonance region, $W<1.75$

Table 1
Results of the fit (see text for details) (Because of the nonlinearity of the problem, the rounding errors can increase the χ^2/ndf up to 1.5). The error estimates have been obtained from a MINOS analysis of the MINUIT program. When the errors are either very asymmetric (denoted by an additional sign) or very different for the pomeron and reggeon terms two numbers are quoted.

Parameters	$\sigma_T(\gamma p)+\sigma_T(\gamma^* p)$		$\sigma_T(\gamma^* p)(1+R)$		Error estimate (%)
m_0^2 (GeV^2)	0.30508		0.30508		15
$m^2_{\mathbb{P}}$ (GeV^2)	10.67564		10.67564		30
$m^2_{\mathbb{R}}$ (GeV^2)	0.20623		0.20623		+60, −25
Λ^2 (GeV^2)	0.06527		0.06527		-
Q_0^2 (GeV^2)	0.27799		0.27001		20
Parameters	Pomeron	Reggeon	Pomeron	Reggeon	Error estimate (%)
a_1	−0.04503	0.60408	−0.04503	0.60408	15
a_2	−0.36407	0.17353	−0.41254	0.08144	10($\mathbb{P}$), 40($\mathbb{R}$)
a_3	8.17091	1.61812	7.54998	2.18355	30
b_1	0.49222	1.26066	0.34131	1.21849	20
b_2	0.52116	1.83624	0.58400	1.82378	20
b_3	3.55115	0.81141	3.25216	0.71033	15
C_1	0.26550	0.67639	0.26550	0.67639	15
C_2	0.04856	0.49027	0.10525	0.52072	100($\mathbb{P}$), 25($\mathbb{R}$)
C_3	1.04682	2.66275	5.55143	1.90782	15

GeV, described by the parametrization of Brasse et al. [21]. It is also of interest to compare the extrapolation of our parametrization to higher values of Q^2, where no data are available, to the predictions of some parametrizations obtained as a result of the evolution of parton densities through the standard QCD evolution equations. The only parametrization valid at low Q^2 is the dynamical parametrization of Glück, Reya and Vogt (GRV) [22] which is applicable above $Q^2=0.3$ GeV^2. For the sake of comparison, among the various other parametrizations [23] we have chosen the KMRS one [24], based on the BCDMS data with an $x^{-0.5}$ behavior for the gluon distribution at low x and a MT parametrization [25] with a sharp rise of all parton distributions at low x as well. Those two, valid above $Q^2=4$ GeV^2, are the ones that predict the fastest rise of F_2 with Q^2 at low x. All the parametrizations to which we compare ourselves have been obtained in a next to leading order approximation. The comparison of the four parametrizations is presented in fig. 4. The largest differences between the various parametrizations are observed for $x<0.015$. The shape of $F_2(x, Q^2)$ predicted by our parametrization seems to develop a wiggle in the region $1<Q^2<10$ GeV^2. We have checked that this wiggle is to a large extend induced by the relative normalization of the NA28 data and the BCDMS data in the region of relatively low x. It is directly linked to the behavior of $a_{I\!P}$ as a function of Q^2 (see below) and was found to be insignificant within the errors of the parameters. We have checked that indeed an increase of the normalisation of the NA28 data by 10% (as suggested by the new, yet unpublished, NMC data [26]) would smooth the wiggle without changing substantially the behavior of $a_{I\!P}$ as a function of Q^2. The GRV parametrization predicts too fast a rise at low Q^2, while no constraints from the data exist for the standard parametrizations. In general, at higher Q^2 the KRMS parametrization lies below the other three, which agree among themselves at least in magnitude. In the intermediate x region, $0.024<x<0.275$, the agreement between the various parametrizations is quite good, but for the low Q^2 region, where that of GRV lies above the data. At the highest Q^2 values our parametrization predicts a faster dependence on Q^2, but our extrapolation, based on an ad hoc Q^2 dependence of some of the terms in the fit, may be unreliable, since no constraints exist from the data in this region. In the high x region, only our parametrization describes properly the whole region of x and Q^2. Clearly, the simple phenomenological picture that underlies our approach may not be sufficient to describe the whole of the $[x, Q^2]$ plane, especially since the functional Q^2 dependence of some terms used in our parametrizations is unknown. The fact that it extrapolates smoothly into the region of higher Q^2 values, where the standard approach may take over, makes it, together with the existing parametrization of the resonance region [21], a very useful tool for estimates in which the low Q^2 region plays an important role.

Another practical consequence of this parametrization is that it can be used to set initial conditions for the standard QCD evolution equations. Indeed, both the absolute value of F_2 and its logarithmic derivative $\mathrm{d}F_2/\mathrm{d}\ln Q^2$ can be determined at any value of Q_0^2 suitable to start a QCD type of evolution. The fact that higher twist contributions can be handled is another asset. The indication that our parametrization may provide good initial conditions can be inferred from fig. 5, where $a_{I\!P}$ and $a_{I\!R}$ have been plotted as a function of Q^2. From the solution of the evolution equation valid at small x [27], $F_2(x, Q^2)$ is expected to be proportional to x^{ω_0}, where ω_0 is derived from the intercept of the bare pomeron pole in perturbative QCD. In the approximation in which the running of the strong coupling constant α_s is neglected, the following limits on ω_0 can be derived [18]:

$$-\frac{3\alpha_s(k_0^2)}{\pi}4\ln 2\leqslant\omega_0\leqslant-\frac{3.6\alpha_s(k_0^2)}{\pi}, \qquad (25)$$

where k_0^2 is some large scale, such that perturbative QCD is applicable. Our fit suggests that the transition between the standard pomeron and the QCD bare pomeron takes place in the region $1\leqslant Q^2\leqslant 10$ GeV^2. For a scale $k_0^2=10$ GeV^2 we expect

$$-0.6\leqslant\omega_0\leqslant-0.26, \qquad (26)$$

which seems to be born out by our fit.

The transition region between a small value of $a_{I\!P}$ as expected from the Regge phenomenology and rising total cross sections and a larger one expected in QCD, is determined by the data, especially by the low x NA28 and BCDMS data. Although the detailed description of the transition is partly dictated by our

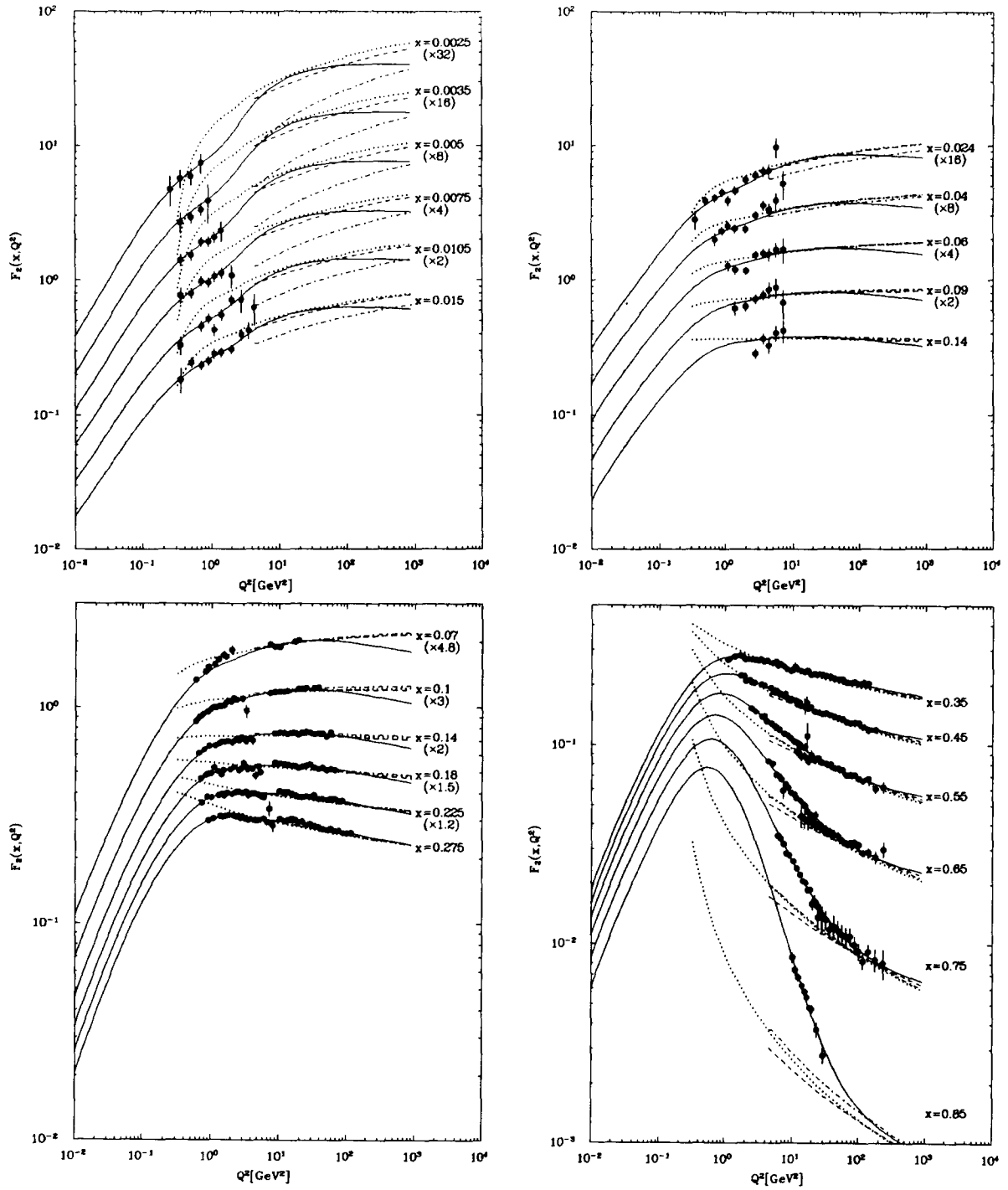

Fig. 4. Comparison of the prediction of our parametrization (full line) with the predictions of the dynamical GRV (dotted line), the KMRS (dash-dotted line) and the MT (dashed line) parametrizations for F_2 as a function of Q^2, for fixed values of x (see the text for more details). The data are superimposed to underline the kinematical region probed by measurements.

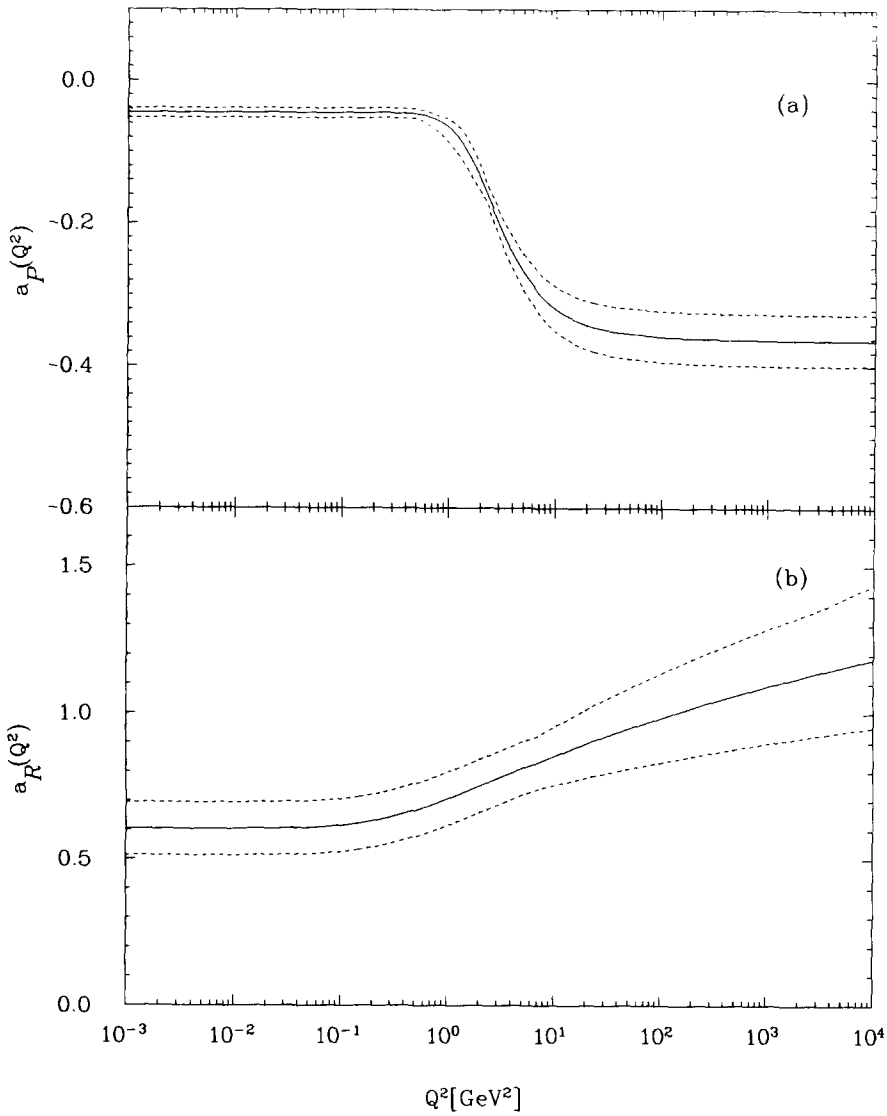

Fig. 5. The Q^2 dependence of the powers $a_{I\!P}$ (a) and $a_{I\!R}$ (b) of $x_{I\!P}$ and $x_{I\!R}$ respectively in the parametrization of the structure function contribution to the cross section for γ^*p interactions. The dashed lines represent the estimated errors.

parametrization of $a_{I\!P}$ as a function of Q^2, it seems to be supported by the data, as well as the fact that both at $Q^2 \leqslant 1$ GeV^2 and $Q^2 > 10$ GeV^2, $a_{I\!P}$ depends only weakly on Q^2. The exact value of $a_{I\!P}$ depends on the normalization of the data, but even in the region of low Q^2 where the NA28 data are determinant, a 10% change of the normalization, which may change the value of $a_{I\!P}$ by 50%, will not change the general picture of the transition region. Similar expectations, as the one obtained in our fit, have been deduced by Collins [28].

The existence of such a transition region, if confirmed by more precise data, as the one expected from HERA, has an interesting implication for the behavior of $\sigma_T(x, Q^2)$ as a function of Q^2 for fixed values of x. This is shown in fig. 6. For sufficiently small values of x, such that the pomeron contribution determines the cross section, after a sharp decrease the

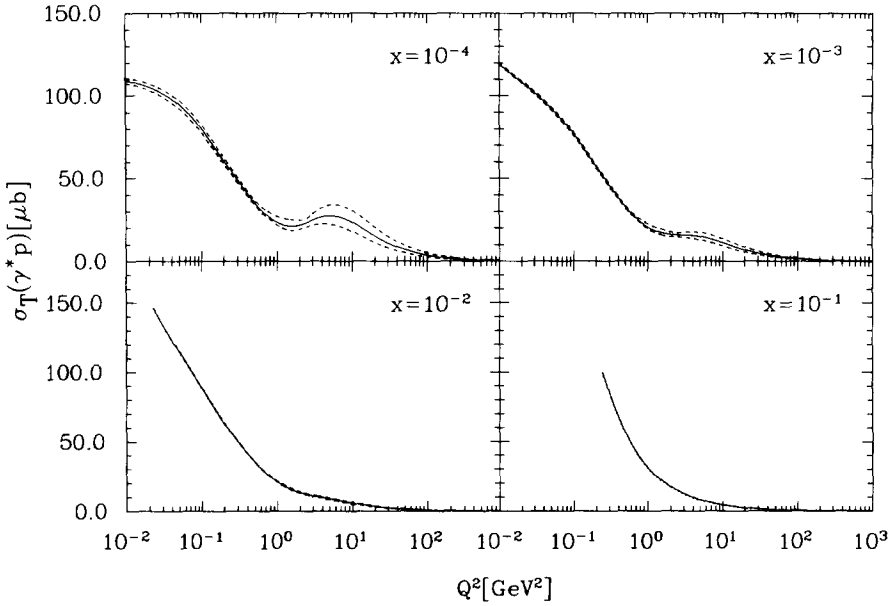

Fig. 6. The Q^2 dependence of the total γp absorption cross section for transversely polarized virtual photons γ* inferred from our parametrization for fixed values of x, indicated on the figure. The dashed lines represent the estimated error.

cross section flattens off in the region of Q^2 between 1 and 10 GeV^2, before it starts falling down again. The detailed shape of the flattening off depends on the description of the transition region observed in the behaviour of $a_{\mathscr{P}}$. The structure (wiggle) that we obtain for small x is a numerical artefact reflecting the need to accommodate both the NA28 and the BCDMS data and is insignificant within error estimates. The flattening of the cross section is a consequence of the sharp decrease of $a_{\mathscr{P}}$ in a relatively small range of Q^2 (see fig. 5a). Whenever the change in $a_{\mathscr{P}}$ is faster than $\ln Q^2$, the flattening is bound to occur. If the region where the cross section flattens off is interpreted as due to some intermediate confined quark states, as appear in some hadron models [29], the radius of a confined quark would be of the order of 0.2 fm, in accordance with other estimates.

It should also be mentioned that our parametrization offers the unique possibility to solve the evolution equation in $\ln(1/x)$ [8] which, for initial conditions, requires the knowledge of $F_2(x, Q^2)$ at a fixed value of $x=x_0$ in the whole of the Q^2 range. For the first time this Q^2 dependence can be derived from the experimental data.

6. Conclusions

Besides a practical advantage of having a parametrization of F_2 that interpolates smoothly between $Q^2=0$ and the DIS region, the fact that one could obtain such a parametrization, based on phenomenological arguments, may indicate that there is indeed a smooth transition between the nonperturbative and perturbative regime described by a Regge type of approach.

The fact that some properties of our parametrization seem to fulfil the general expectations is very encouraging and we hope that this kind of approach that we intend to pursue may lead to a better understanding of the connection between the phenomenology and theoretical predictions, especially in the region of small x. The forthcoming HERA results, which are expected to populate the low x region at relatively high Q^2 values will certainly be very valuable.

Acknowledgement

We are indebted to G. Wolf for a careful and critical reading of this paper. We are grateful to K. Charchula for providing us with the curves for the stan-

dard QCD and the dynamical parametrizations. Three of us (H.A., E.M.L., A.L.) would like to thank the DESY Directorate for supporting their stays at DESY. One of us (U.M.) would like to thank the Minerva Foundation for the financial support which made his stay at DESY possible. This work was partly supported by the German Israeli Foundation (GIF I-149-10.7/89) and by the Polish Ministry of Education (GMEN 133/90).

References

[1] R.J.M. Cotvolan and E. Predazzi, in: Problems of fundamental modern physics, eds. R. Cherubini, P. Dalphiaz and B. Minetti, (World Scientific, Singapore, 1991) p. 85.
[2] G. Wolf, Proc. 1971 Intern. Symp. on Electron and photon interactions at high energies (Cornell, 1971) p. 189.
[3] A. Levy and U. Maor, Phys. Lett. B 182 (1986) 108.
[4] A.J. Buras and K.J.F. Gaemers, Nucl. Phys. B 132 (1978) 249.
[5] C. Lopez and F.J. Yndurain, Nucl. Phys. B 171 (1980) 231; B 183 (1981) 157.
[6] F. Martin, Phys. Rev. D 19 (1979) 1382.
[7] Yu.L. Dokshitzer, D.I. Dyakonov and S.I. Troyan, Phys. Rep. 58 (1980) 269.
[8] L.V. Gribov, E.M. Levin and M.G. Ryskin, Phys. Rep. 100 (1983) 1.
[9] U. Maor and E. Gotsman, Phys. Rev. D 28 (1983) 2149.
[10] A. Donnachie and P.V. Landshoff, Nucl. Phys. B 224 (1984) 322.
[11] V.S. Fadin, E.A. Kuraev and L.N. Lipatov, Phys. Lett. B 60 (1975) 50; JETP 72 (1977) 377.
[12] M. Arnedo et al., Nucl. Phys. B 333 (1990) 1.
[13] A.C. Benvenuti et al., Phys. Lett. B 223 (1989) 485.
[14] L.W. Whitlow, Ph.D. Thesis, SLAC-report-357 (1990).
[15] D. Allasia et al., Phys. Lett. B 249 (1990) 366.
[16] L.W. Whitlow et al., Phys. Lett. B 250 (1990) 193.
[17] L.N. Lipatov, Sov. Phys. JETP 63 (1986) 904.
[18] J.C. Collins and J. Kwieciński, Nucl. Phys. B 136 (1989) 307.
[19] A. Milsztajn et al., preprint CERN-PPE/90-135.
[20] A. Donnachie and P.V. Landshoff, Phys. Lett. B 207 (1988) 319.
[21] F.W. Brasse et al., Nucl. Phys. B 110 (1976) 413.
[22] M. Glück, E. Reya and A. Vogt, preprint DO-TH-91/07, submitted to Z. Phys.
[23] K. Charchula, M. Krawczyk, H. Abramowicz and A. Levy, preprint DESY 90-019.
[24] J. Kwieciński, A.D. Martin, R.G. Roberts and W.J. Stirling, Phys. Rev. D 42 (1990) 3645.
[25] J.G. Morfin and W.K. Tung, preprint Fermilab-Pub-90/74.
[26] I.G. Bird, (NM Collab.), preliminary results, presented LP-HEP91 Conf. (Geneva, 1991).
[27] Ya.Ya. Balitzkij and L.N. Lipatov, Yad. Fiz. 28 (1978) 1597.
[28] J.C. Collins, Proc. 7th Topical Workshop on Proton–antiproton collider physics (June 1988).
[29] E.M. Levin and M.G. Ryskin, Phys. Rep. 189 (1990) 267.